Displacive transition in magnesiowüstite

2002 J. Phys.: Condens. Matter 14 11349

(http://iopscience.iop.org/0953-8984/14/44/480)

INSTITUTE OF PHYSICS PUBLISHING JOURNAL OF PHYSICS: CONDENSED MATTER

J. Phys.: Condens. Matter **14** (2002) 11349–11354 PII: S0953-8984(02)38299-7

Displacive transition in magnesiowüstite

Wendy Mao, Jinfu Shu, Jingzhu Hu, Russell Hemley and Ho-kwang Mao

Geophysical Laboratory and Center for High Pressure Research, Carnegie Institution of Washington, 5251 Broad Branch Road, NW, Washington, DC 20015, USA

E-mail: w.mao@gl.ciw.edu

Received 18 June 2002
Published 25 October 2002
Online at stacks.iop.org/JPhysCM/14/11349

Abstract

Magnesiowüstite $(Mg_{0.1}Fe_{0.9})O$ was studied at ambient temperature under both hydrostatic and quasihydrostatic pressures to 35 GPa. The elastic behaviour, equation of state, transition pressure, and the structure before and after the B1–rhombohedral transition were determined. K_0- and K_0'-values for the B1 phase were calculated to be 155 ± 10 and 3.6 ± 0.8 GPa respectively under hydrostatic conditions. The second-order B1–rhombohedral transition occurred at 20 GPa. Quasihydrostatic conditions were used to determine the stress/strain in different crystallographic directions to elucidate the transition mechanism which is triggered by the softening of the c_{44} in the B1 phase.

(Some figures in this article are in colour only in the electronic version)

1. Introduction

The behaviour of magnesiowüstite is of considerable significance for understanding the Earth's deep interior. Olivine, the major mineral in the upper mantle, decomposes into silicate perovskite and magnesiowüstite in the lower mantle. Studies on the partitioning of Mg and Fe in the lower mantle [1, 2] point to a magnesium rich composition for magnesiowüstite. Oxygen is a candidate light element in the liquid outer core, which is therefore thought to have a high FeO content. The D″ layer is a possible reaction zone between the MgO rich lower mantle and the FeO rich outer core. An understanding of the elastic behaviour of magnesiowüstite would help to explain the seismic anisotropy that is observed in this layer. At ambient conditions, both end members of magnesiowüstite, MgO and FeO, are in the cubic rock-salt structure, have very similar lattice parameters, and form a complete solid solution. However, they display very different high-pressure behaviour. MgO does not undergo any phase transitions to at least 227 GPa [3], and while it is slightly elastically anisotropic at low pressure it becomes increasingly isotropic as pressure increases [4]. In contrast, FeO undergoes a number of phase transitions from the B1 to rhombohedral to NiAs structure [5, 6]. The B1–rhombohedral phase transition shown in figure 1 [7] appears to be a displacive transition.

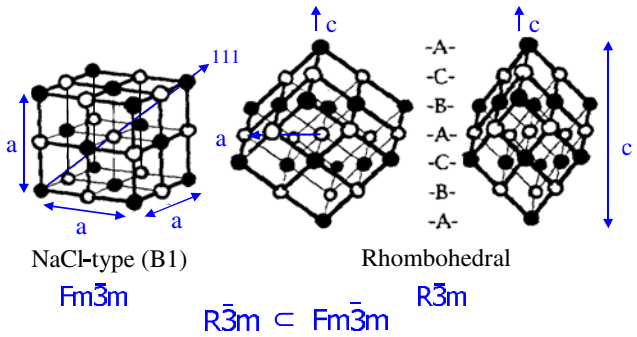

Figure 1. B1–rhombohedral transition of FeO.

For such a transition, one can apply the Landau theory of second-order phase transitions. One of the necessary conditions is the Landau subgroup criterion which requires that the low-symmetry phase be a subgroup of the high-symmetry phase. This criterion is met in the case of the phase transition from the B1 (space group $Fm\bar{3}m$) to the rhombohedral ($R\bar{3}m$) state in wüstite. The phase transition involves the distortion of the cubic structure by the compression of three cubic body diagonals. The observed softening of the c_{44}-modulus of the B1 phase, which favours the deformation of the body diagonals, is related to magnetic effects [8]. While wüstite is elastically isotropic at ambient pressure it becomes highly anisotropic as pressure increases [9–11]. In this study we investigated the phase transitions and elasticity of an intervening composition of magnesiowüstite near the iron end member.

2. Experimental details

Experiments were conducted in a diamond anvil cell. A 150 μm hole was drilled in a stainless steel gasket into which the polycrystalline $(Mg_{0.1}Fe_{0.9})O$ sample was placed. Ruby chips were added for pressure calibration and to gauge the degree of hydrostaticity. Helium was used as the pressure transmission medium in the hydrostatic experiment and was partially bled for the quasihydrostatic experiment in which the anvils approached the sample and caused uniaxial differential stress. Polychromatic (white) synchrotron x-radiation at X17C superconducting-wiggler beamline of the National Synchrotron Light Source (NSLS) was used for energy-dispersive x-ray diffraction (EDXD) measurements. The incoming x-ray, beam size 20 μm, was directed through the diamond axis, and the diffracted beam was collected with a Ge solid-state detector at a fixed 2θ angle of 15° (figure 2). The diffracting planes, as represented by the arrow in the strain ellipse in figure 2, were at $90° - \theta$ to the compressional axis. Under hydrostatic conditions, the strain ellipse becomes a circle. Under non-hydrostatic conditions, the strain is maximum along the diamond axis, and minimum perpendicular to the diamond axis. Since the planes sampled in this study had normals nearly perpendicular to the diamond axis, under non-hydrostatic conditions the planes experienced less strain and had larger d-spacings relative to those under hydrostatic conditions.

3. Results and discussion

Three representative x-ray diffraction patterns and ruby fluorescence spectra taken under hydrostatic and quasihydrostatic conditions are shown in figure 3. The bottom pattern was taken at 19.3 GPa under hydrostatic compression just below the transition pressure. The cubic 111,

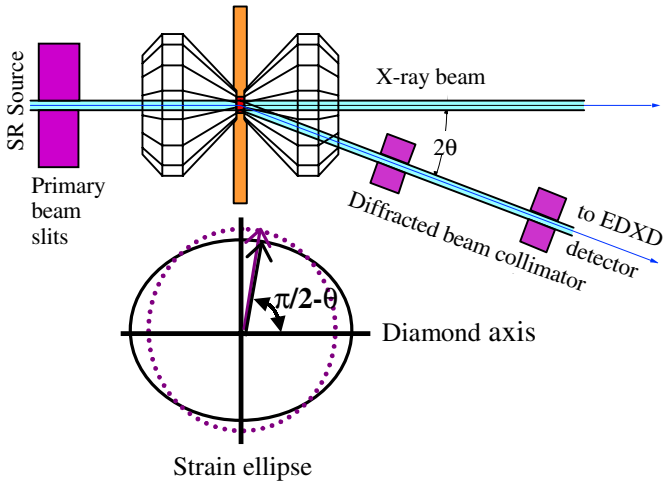

Figure 2. Schematic diagram of the EDXD set-up with the resulting strain ellipse. The arrow represents the diffracting plane normal. The circle shows the strain ellipse under hydrostatic conditions; the ellipse with semimajor axis along the diamond axis shows the strain ellipse under quasihydrostatic conditions.

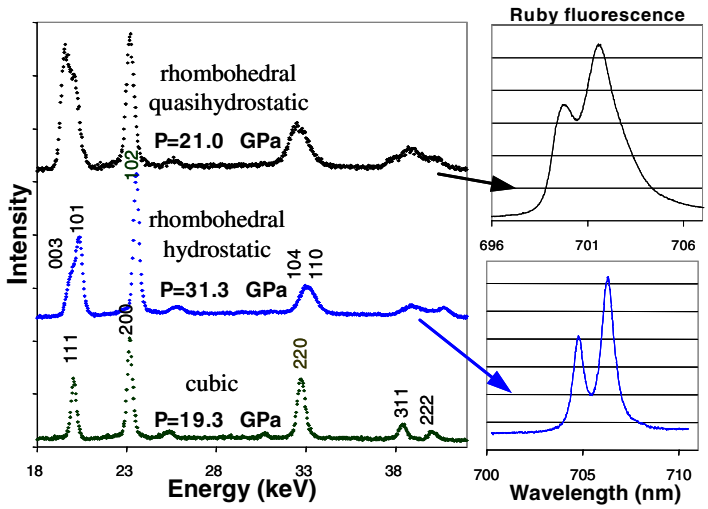

Figure 3. EDXD patterns and ruby fluorescence spectra taken under hydrostatic and quasihydrostatic conditions.

200, 220, 311, and 222 peaks fit a cubic cell perfectly. The middle pattern was taken under hydrostatic conditions at 31.3 GPa. The sample has transformed into the rhombohedral phase which can be seen by the splitting of the cubic 111 into the rhombohedral 003 and 101 peaks. The expected 1:3 intensity ratio between the 003 and 101 peaks is also observed. The cubic 200 does not split and becomes the rhombohedral 102 singlet. The ruby spectra shows that the conditions are hydrostatic as demonstrated by the well-resolved R_1 and R_2 fluorescence peaks. The top pattern shows the sample in the rhombohedral phase under quasihydrostatic conditions as indicated by the broadening of the R_1 and R_2 peaks. The 003 peak has grown relative to

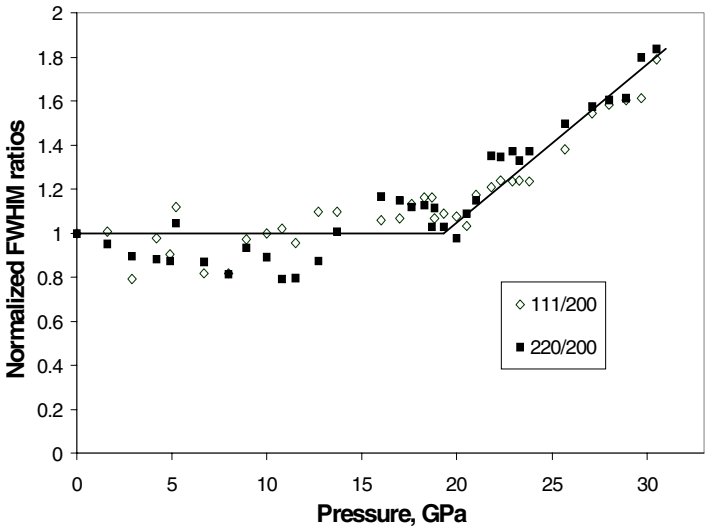

Figure 4. Normalized FWHM ratios versus pressure for the cubic 111 and 220 peaks under hydrostatic conditions. The transition pressure was determined by finding the point where these peaks start splitting as seen by an increase in the normalized FWHM ratio from its ideal cubic value of one.

the 101 because of preferred orientation which develops under uniaxial stress. The longer body diagonal, the rhombohedral 003, tends to lie in the direction of lowest strain which is approximately the direction being sampled.

The evolution from cubic to rhombohedral under hydrostatic conditions was followed by examining the broadening and splitting of the cubic 111 and 220 peaks. The values for the peak widths were normalized to take into consideration factors like instrumentation and energy resolution and compared to the width of the 200 peak which does not split. For the cubic phase, the ratios should be unity, but as the rhombohedral phase produces the broadening and eventual splitting of peaks, these ratios increase. The transition pressure was determined by extrapolating back from higher pressures and was found to occur at 20 GPa (figure 4).

Pressure–volume data are shown in figure 5. The cubic data were fitted with a second-order Birch–Murnaghan equation of state (EOS) up to the transition point, giving K_0 and K_0' of 155 ± 10, 3.6 ± 0.8 GPa respectively, which are in good agreement with published values [12]. The rhombohedral data are shown by the open triangles; no volume discontinuity is seen, consistent with a continuous transition. The closed symbols show results under quasihydrostatic conditions after some helium was bled out. The quasihydrostatic conditions result in larger volumes (d-spacings are larger than those under hydrostatic conditions as explained previously). Under hydrostatic conditions the phase transition was reversible, but under quasihydrostatic conditions the rhombohedral phase was still seen down to 9 GPa. The transition pressure is clearly very sensitive to any degree of non-hydrostaticity.

Comparing a series of planes lying in the a–c plane, the effect of non-hydrostatic stress is strikingly different in different crystallographic conditions. The rhombohedral 003 is strongly affected by non-hydrostatic stress while the 102 is the least affected. Figure 6 shows a plot of $\Delta d/d$ versus B. $\Delta d/d$ is the difference in d-spacing under quasihydrostatic and hydrostatic

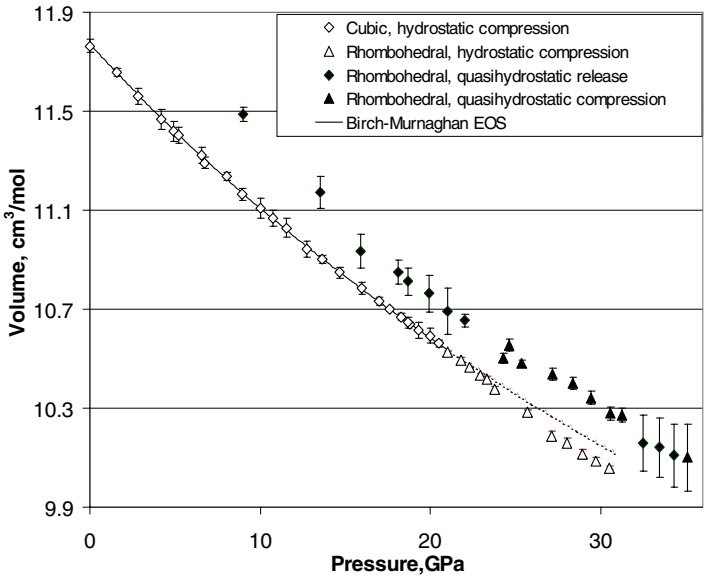

Figure 5. Pressure–volume data.

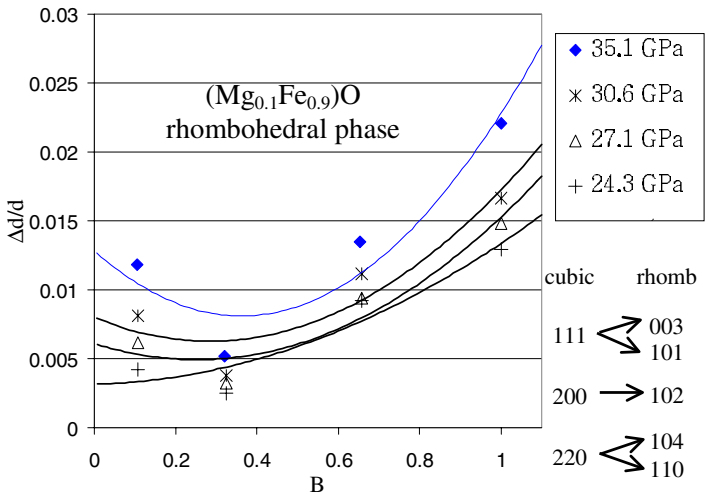

Figure 6. $\Delta d/d$ versus B for four pressures in the rhombohedral phase. The table bottom left shows a list of relevant cubic peaks and the rhombohedral peaks they transform into.

conditions for a given pressure:

$$\frac{\Delta d}{d} = \frac{d_{quasi} - d_{hydro}}{d_{hydro}}.$$

B is the angular variation in the a–c plane given by the following relation [13]:

$$B = \frac{3a^2l^2}{[4c^2(h^2 + hk + k^2) + 3a^2l^2]}$$

where hkl refer to crystallographic indices. The large $\Delta d/d$ for 003 (i.e. the rhombohedral c-axis which was originally the cubic 111 body diagonal) means that it was the most deformable

direction, especially compared to the stiff 102 which was originally the cubic a-axis. A soft cubic 111 means a soft elasticity tensor element c_{44} in the cubic phase which triggers the B1–rhombohedral transition as in the case of pure FeO [7].

4. Conclusions

The EOS for the cubic B1 phase of $(Mg_{0.1}Fe_{0.9})O$ was determined up to 20 GPa. The B1 phase transforms into a rhombohedral phase at 20 GPa, an increase from 17 GPa for pure FeO. The transition pressure is very sensitive to the degree of hydrostaticity. Quasihydrostatic conditions are usually thought of as undesirable, but in conjunction with hydrostatic data, they provide rich, additional information. In this case we were able to gain insight into the transition which is triggered by the softening of the c_{44} in the cubic phase.

Acknowledgments

We thank Agnes Mao for her help and encouragement. We also thank NSLS (supported by DOE) for providing synchrotron beamtime and NSF for financial support.

References

[1] Mao H-K, Shen G and Hemley R J 1997 *Science* **278** 2098
[2] Andrault D 2001 *J. Geophys. Res.* **106** 2079
[3] Duffy T S, Hemley R J and Mao H-K 1995 *Phys. Rev. Lett.* **74** 1371
[4] Zha C-S, Mao H-K and Hemley R J 2000 *Proc. Natl Acad. Sci. USA* **97** 13 494
[5] Zou G *et al* 1980 *Carnegie Inst. Washington Yearb.* **79** 374
[6] Fei Y and Mao H-K 1994 *Science* **266** 1678
[7] Mao H-K *et al* 1996 *Phys. Earth Planet. Int.* **96** 135
[8] Struzhkin V V *et al* 2002 *Phys. Rev. Lett.* **87** 255501
[9] Jacobsen S D *et al* 2002 *J. Geophys. Res.* **107** 10, 1029/2001 JB000490
[10] Jackson I *et al* 1990 *J. Geophys. Res.* **95** 671
[11] Singh A K *et al* 1998 *Phys. Rev. Lett.* **80** 2157
[12] Richet P, Mao H-K and Bell P M 1989 *J. Geophys. Res.* **94** 3037
[13] Singh *et al* 1998 *J. Appl. Phys.* **83** 7567